THE JOURNAL OF PHYSICAL CHEMISTRY Letters

Letter

Cite This: J. Phys. Chem. Lett. 2019, 10, 1763−1768

pubs.acs.org/JPCL

Accurate Probabilities for Highly Activated Reaction of Polyatomic Molecules on Surfaces Using a High-Dimensional Neural Network Potential: CHD_3 + Cu(111)

N. Gerrits,*,† Khosrow Shakouri,† Jörg Behler,‡ and Geert-Jan Kroes*,†

†Gorlaeus Laboratories, Leiden Institute of Chemistry, Leiden University, P.O. Box 9502, 2300 RA Leiden, The Netherlands

‡Institut für Physikalische Chemie, Theoretische Chemie, Universität Göttingen, Tammannstrasse 6, 37077 Göttingen, Germany

Supporting Information

ABSTRACT: An accurate description of reactive scattering of molecules on metal surfaces often requires the modeling of energy transfer between the molecule and the surface phonons. Although ab initio molecular dynamics (AIMD) can describe this energy transfer, AIMD is at present untractable for reactions with reaction probabilities smaller than 1%. Here, we show that it is possible to use a neural network potential to describe a polyatomic molecule reacting on a mobile metal surface with considerably reduced computational effort compared to AIMD. The highly activated reaction of CHD_3 on Cu(111) is used as a test case for this method. It is observed that the reaction probability is influenced considerably by dynamical effects such as the bobsled effect and surface recoil. A special dynamical effect for CHD_3 + Cu(111) is that a higher vibrational efficacy is obtained for two quanta in the CH stretch mode than for a single quantum.

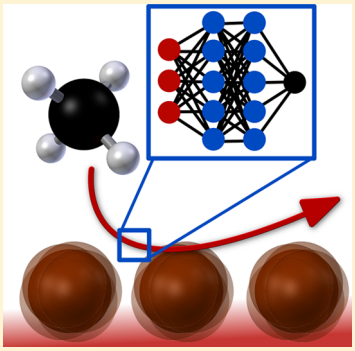

Accurately describing molecule−surface reactions is of vital importance for the understanding of heterogeneously catalyzed processes such as the Haber−Bosch[1] and steam reforming processes.[2] Unfortunately, the complexity of the interaction between molecules and metals limits the accuracy of theoretical studies on these kinds of processes.[3−8] Often, chemically accurate results are obtainable at high computational cost with ab initio molecular dynamics (AIMD) combined with the so-called Specific Reaction Parameter (SRP) approach.[9−11] However, the investigation of reactions with low reactivity (<1%) remains challenging due to the need for a large number of trajectories in combination with a large computational cost.[12] Therefore, neural network approaches have recently been employed in order to obtain results with the accuracy of AIMD using density functional theory (DFT), but with a considerably smaller computational cost.[13−18] So far, these studies either involved diatomic molecules[15−17,19] or they neglected the movement of surface atoms.[18,20−23] Very recently, a high-dimensional neural network potential (HD-NNP) has been developed for a system in which a linear triatomic molecule interacts with a metal surface, i.e., CO_2 + Ni(100),[24] also including surface atom motion. The neglect of surface motion can limit the accuracy of these studies due to the neglect of energy exchange between the molecule and the surface.[4,12,17,19,25−30] This lack of energy exchange represents a severe approximation for the dynamics of polyatomic molecules reacting on metal surfaces due to their high mass.[31,32] A modified Shepard interpolation method[33] has also been used to describe the potential of a polyatomic molecule reacting on a metal surface but again with the neglect of surface motion. Reactive force field fits have been made that do include surface motion,[34,35] but the quality of these fits remains unclear. However, no neural network potential has been employed so far for nonlinear polyatomic molecules interacting with surfaces that explicitly includes the effect of surface motion as well.

In this work, we focus on the dissociative chemisorption of CHD_3 on Cu(111) because the system exhibits a low reactivity,[12] making reactive AIMD studies untractable for most incidence energies achievable in molecular beams. Moreover, high-quality graphene can be synthesized using methane dissociation on copper,[36−42] and this warrants additional study of the rate-controlling step, namely, the breaking of the first CH bond. The Eley−Rideal reaction of D with CD_3 preadsorbed on Cu(111) has also been studied.[43] The methane + Cu(111) system shows interesting dynamics in that the low reactivity of methane on Cu(111) is not only caused by a high barrier (167 kJ/mol) but also by specific features of the potential energy surface (PES) such as the curvature of the minimum energy path (MEP).[12] For all of these reasons, we apply the neural network Behler−Parrinello approach[13,14] for the first time to a nonlinear polyatomic molecule reacting on a metal surface, which makes accurate simulations feasible while including surface motion, using CHD_3 + Cu(111) as an example.

In the HD-NNP, the total energy is evaluated as a sum of atomic contributions that are dependent on their energetically relevant local environment, which is described by many-body

Received: February 26, 2019
Accepted: March 28, 2019
Published: March 28, 2019

DOI: 10.1021/acs.jpclett.9b00560
J. Phys. Chem. Lett. 2019, 10, 1763−1768

atom-centered symmetry functions.[44] In total, 38 000 DFT data points were used to train the HD-NNP, of which 14 000 points were taken from an AIMD study.[12] Other data points included structures sampling the van der Waals well and transition state regions and the molecule's vibrational modes. Finally, dynamically important structures missing from the data set were identified by running molecular dynamics (MD) on the (incomplete) HD-NNP and then added to the data set in a procedure described in ref 14. For the neural network, two hidden layers were used, each with 15 nodes. The training was carried out using the RuNNer code,[45−47] and the MD was performed with LAMMPS.[48,49]

First, the accuracy of the HD-NNP is tested by comparing the 2D elbow plot of methane on Cu(111) in which methane is fixed in all molecular coordinates according to its transition state geometry, as depicted in Figure 1a, except for Z and r (the distance between the carbon and surface and the length of the dissociating CH bond). The HD-NNP is compared directly with DFT calculations in Figure 1b. Here we see that the HD-NNP reproduces the DFT data remarkably well, even though points from the 2D cut are not included in the data set. When the methane is relaxed in all degrees of freedom other than r and Z (Figure 1c), the MEP lies slightly closer to the surface than to the MEP of the constrained methane. Again, the HD-NNP reproduces the direct DFT calculations quite well. Moreover, both the electronic and mechanical coupling[32] are in good agreement with DFT (see Figure 1d,e), which means that changes in the barrier height and geometry with respect to the motion of the surface atom below the dissociating molecule are described correctly. Furthermore, using 90% of the DFT data set as the training set and 10% as the test set, the root-mean-square error (RMSE) is 1.7 kJ/mol for the test set, which is well within chemical accuracy (4.2 kJ/mol). (Note that all errors reported in this work are with respect to the full system, i.e., the total energy.) The high fitting accuracy is also observed in Figure 2, where the distributions of the absolute error for the training and test set are shown and the vast majority of the errors falls within chemical accuracy. The total energy for all of the structures in the training and test set obtained with the HD-NNP and direct DFT calculations is also shown in Figure S1. Moreover, the RMSE for the forces in the test set is 2.3 kJ/mol/Å. The RMSE of 1.7 kJ/mol that we obtain here on the basis of 38 000 DFT points for CHD_3 + Cu(111) with the surface atoms allowed to move compares well with the RMSE of 1.5 kJ/mol obtained for a recent 15D NN static surface PES for CHD_3 + Ni(111) on the basis of 200 000 DFT points.[22,30] We also note that the approximate modified generalized Langevin oscillator method used in ref 30 to effectively add surface atom motion to the problem may run into problems if the molecule−surface interaction depends on more than just one surface atom coordinate, as for instance is the case for H_2O + Ni(111)[50] and may be the case for methane interacting with stepped metal surfaces.[30]

The goal is to make a HD-NNP that is capable of accurately evaluating the energy and forces on the fly during MD simulations. Therefore, not only are incidence energies with low reaction probabilities (<1%) investigated but also regimes with higher reaction probabilities that are obtainable with AIMD in order to test the validity of the results obtained with the HD-NNP. Figure 3 shows the results obtained for the dissociative chemisorption of CHD_3 on Cu(111) with MD using the HD-NNP and with AIMD[12] by simulating a molecular beam for the rovibrational ground state and under laser-off and laser-on conditions. Under laser-off conditions, the molecular beam's vibrational state population is sampled according to the nozzle temperature, and under laser-on conditions, the CH stretch mode ν_1 is excited with one or two

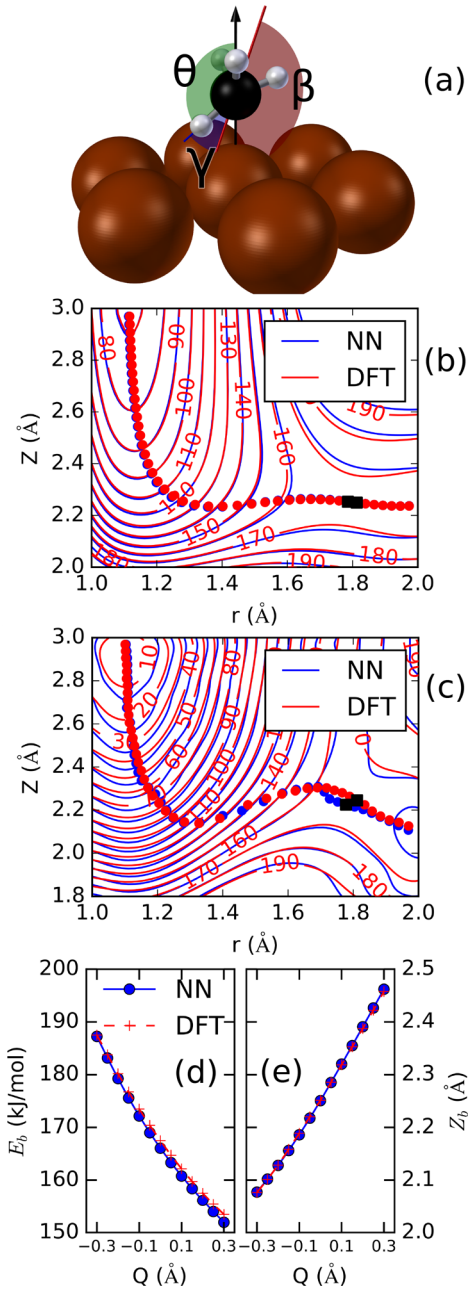

Figure 1. (a) Transition state geometry of methane on Cu(111), indicating the θ, β, and γ angles. (b) Elbow plot of methane on Cu(111) as a function of Z and r (distance between the carbon and surface and bond length of the dissociating hydrogen, respectively), where other degrees of freedom are fixed according to the transition state geometry. Contour lines are drawn at intervals of 10 kJ/mol between 0 and 200 kJ/mol. The blue and red lines are NN and DFT results, respectively. The circles indicate the MEP. (c) Same as (b) but with all degrees of freedom of the methane relaxed, except Z and r. (d) Variation of the barrier height as a function of the vertical displacement Q of a top layer Cu atom. (e) Vertical shift of the barrier location as a function of the vertical displacement Q of a top layer Cu atom.

DOI: 10.1021/acs.jpclett.9b00560
J. Phys. Chem. Lett. 2019, 10, 1763−1768

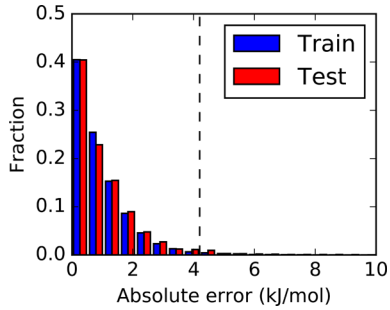

Figure 2. Distribution of absolute total energy errors (kJ/mol) of the HD-NNP compared to the DFT total energy. Blue indicates the training set, whereas red indicates the test set. The dashed line indicates chemical accuracy, i.e., 4.2 kJ/mol.

quanta. In order to describe the reaction probability with good statistics, 10 000−110 000 quasiclassical trajectories were computed per incidence condition. Here we see that at high incidence energy and for vibrationally excited methane, for four sets of initial conditions resulting in reaction probabilities obtained with AIMD, good agreement exists between AIMD and MD performed with the HD-NNP (see also Table 1 and the statistical analysis in the SI). Moreover, reaction probabilities as low as 5×10^{-5} have been computed with the HD-NNP, which was previously not possible using accurate methods. It is observed that at the highest incidence energy (181 kJ/mol) the laser-off simulation yields a similar reaction probability as the $\nu_1 = 1$ simulation, which is caused by the high amount of vibrational excitation in the laser-off beam due to the high simulated nozzle temperature (T_n = 1000 K). However, it should be noted that sticking probabilities computed for laser-off conditions and nozzle temperatures higher than 650 K may be unreliable due to intramolecular vibrational energy redistribution (IVR) among vibrational states in which CD bends and stretches are excited.[9]

Our dynamical simulations show that the reaction of methane is promoted by both translational and vibrational energy. Plotting the reaction probability as a function of the total energy (vibrational + translational energy) shows that putting vibrational energy into the reaction is almost equally or more efficient than increasing the translational energy, depending on the amount of quanta in the ν_1 CH stretch mode (see Figure 3b). The vibrational efficacy is equal to or larger than 0.8, which can be expected for such a late barrier system[51] combined with a MEP of the shape shown in Figure 1c, causing incoming molecules to have to react over considerably higher barriers because they run off of the MEP(the "bobsled effect"[52,53]). This could play a large role at catalytic conditions, where graphene is produced from methane using very high temperatures (>1200 K)[36,41] and thus vibrational excitation is prevalent. Interestingly, the vibrational efficacy[54,55] for the excitation from the $\nu_1 = 1$ to 2 overtone ($\eta_{\nu_1=2,1}$ = 1.7) is considerably higher than that for the excitation from the ground state to $\nu_1 = 1$ ($\eta_{\nu_1=1,0}$ = 0.8). To our knowledge, a higher vibrational efficacy for an overtone has not been observed before.[54−58] In Figure S4, it is observed that when the incidence energy decreases, for $\nu_1 = 2$, reacted trajectories follow the MEP more closely. In Figure 4a, an increase of vibrational energy causes trajectories going on to react to follow the MEP more closely. The dynamical effect (see Figure 4b) is that, because a higher incidence energy is

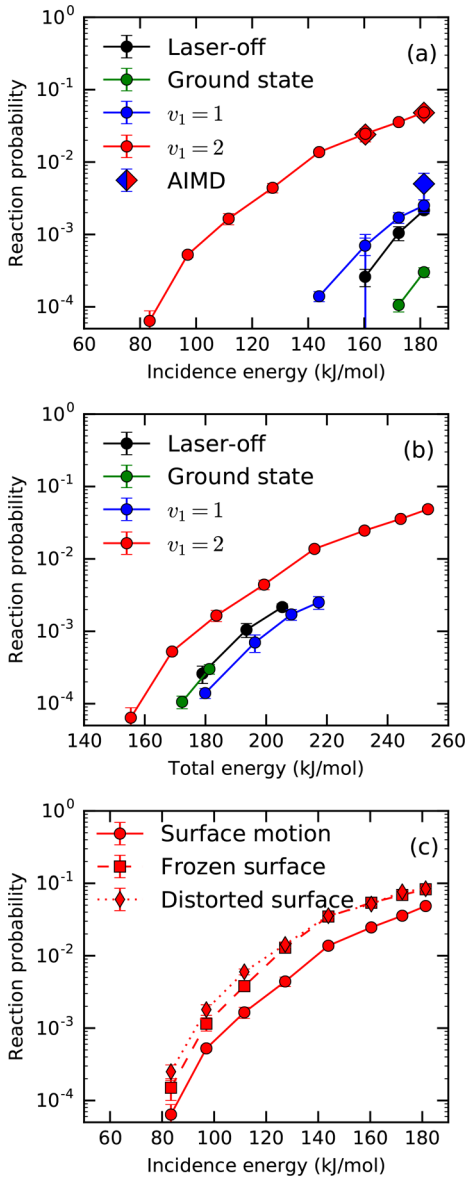

Figure 3. (a) State-selected and molecular beam reaction probabilities of CHD_3 on Cu(111) as a function of the translational energy. Simulations for laser-off (black), rovibrational ground state (green), $\nu_1 = 1$ (blue), and $\nu_1 = 2$ (red), where the circles and diamonds are HD-NNP and AIMD results, respectively. (b) Same as panel (a), but here the reaction probability is shown as a function of the total energy (vibrational + translational energy). (c) Simulations for $\nu_1 = 2$ with (solid line with circles) and without surface motion, where squares with a dashed line indicate an ideal surface and diamonds with a dotted line indicate a thermally distorted surface. The error bars represent 68% confidence intervals.

Table 1. Reaction Probabilities Obtained with the HD-NNP and AIMD[a]

$\langle E_i \rangle$ (kJ/mol)	quantum state ν_1	P_R (HD-NNP)	P_R (AIMD)
160.4	1	0.0007 ± 0.0002	0.000 ± 0.001
160.4	2	0.0246 ± 0.0016	0.024 ± 0.005
181.3	1	0.0025 ± 0.0005	0.005 ± 0.002
181.3	2	0.0486 ± 0.0022	0.048 ± 0.007

[a]The error bars represent 68% confidence intervals.

DOI: 10.1021/acs.jpclett.9b00560
J. Phys. Chem. Lett. 2019, 10, 1763−1768

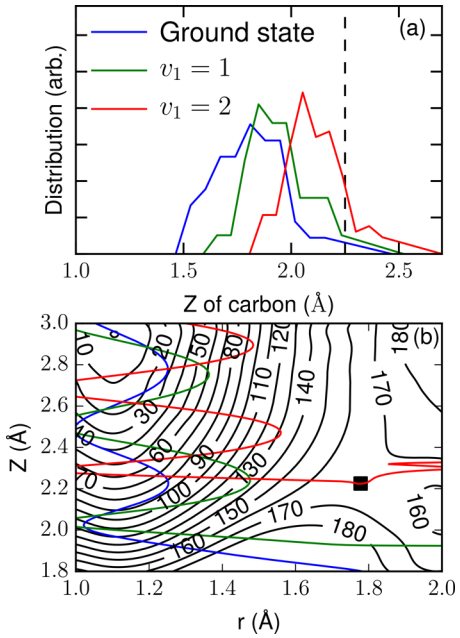

Figure 4. (a) Distributions of the height of the carbon when a hydrogen bond dissociates, i.e., $r = r^{\ddagger}$, for the rovibrational ground state, $\nu_1 = 1$ and 2 at incidence energies with comparable reaction probabilities (about 0.03%). The transition state geometry value for Z is indicated by the dashed line. (b) Elbow plot of methane on Cu(111) obtained with the HD-NNP, where Z and r (distance between the carbon and surface and bond length of the dissociating hydrogen, respectively) are variable and all other degrees of freedom are relaxed. Contour lines are drawn at intervals of 10 kJ/mol between 0 and 180 kJ/mol. Typical trajectories that go on to react for P = 0.03% are indicated by the blue (ground state), green ($\nu_1 = 1$), and red ($\nu_1 = 2$) lines. The black square indicates the highest point along the MEP.

needed to overcome the barrier for a low ν_1, for low ν_1, the carbon atom smashes into the repulsive wall. The hydrogen moves out while the carbon is still close to the surface, and therefore, a higher barrier needs to be overcome (see Figure 4). Hence, a higher vibrational efficacy is observed for $\nu_1 = 2$ because the bobsled effect will be less prominent and thus lower barriers need to be overcome.

We already noted that the reaction probabilities at high incidence energy obtained with the HD-NNP are in good agreement with AIMD. However, the validity of the quasiclassical approximation for the low reaction probabilities needs to be tested by comparison to experiment due to the possibility of quantum effects and potential problems with zero-point energy violation, even though it has been shown that at elevated surface temperature the reaction of methane happens in a "classical over the barrier fashion" with assistance of surface atom motion and without the need for tunneling.[4,59]

The main goal of applying the Behler−Parrinello method to polyatomic molecules is to be able to explicitly include surface motion. Therefore, to evaluate the effect of surface motion, reaction probabilities for $\nu_1 = 2$ have also been computed using a static surface model, where the surface was kept in its ideal relaxed static configuration (note that the lattice expansion corresponding to a surface temperature of 550 K was kept). This effectively removes energy transfer between the molecule and the surface and the corrugation in barrier heights and positions related to surface motion. Reaction probabilities for this frozen surface are a factor 2 higher than those when surface motion is allowed (see Figure 3c). Furthermore, when the distortions of a hot surface are included while still excluding surface motion, i.e., modeling a static thermally disordered surface (similar to the so-called static corrugation model[60]), reaction probabilities are increased by 50% compared to the frozen ideal surface at low incidence energies. At high incidence energies, no difference is observed between the results for the static ideal and the distorted surface, with the latter including the effect of the electronic coupling (or the so-called β-coupling).[32] Our observation that explicitly including surface motion at these high incidence energies lowers the reaction probabilities suggests that the reaction probabilities are decreased due to energy transfer to the surface as the molecule first impacts on the surface (Figure 4b) and possibly also due to surface recoil (mechanical coupling).[4,32] Because the surface recoil effect (which is due to surface atom vibrational averaging) tends to be small,[32] we suspect that the energy transfer is most important. This effect can only be addressed with explicit modeling of the surface motion and not by the sudden and energy averaging methods typically used with quantum dynamics simulations.[32]

To summarize, in this work, the Behler−Parrinello approach was used to develop a HD-NNP that describes a polyatomic molecule reacting on a mobile metal surface, i.e., CHD_3 + Cu(111). The HD-NNP was found to be in good agreement with DFT, which means that MD can be performed with the accuracy of AIMD but with a considerably lower computational effort. Using this HD-NNP, reaction probabilities as low as 5×10^{-5} were obtained, which was untractable with previous accurate methods such as AIMD, while including surface motion. It was found that vibrational excitation plays a major role in the reactivity, where the overtone has a higher vibrational efficacy than the fundamental vibrational excitation. Moreover, allowing energy transfer from the molecule to the surface considerably reduces the overall reactivity. Hence, surface motion needs to be included explicitly in simulations in order to obtain quantitative results for molecular beam simulations of methane reacting on copper. More work is still required to investigate the effect of surface temperature on the reaction of CHD_3 on Cu(111) as we addressed only one surface temperature (550 K). Finally, the quasiclassical approximation needs to be tested for low reaction probabilities by comparison to experiments due to the possibility of quantum effects and zero-point energy violation. However, this would not be an intrinsic problem of the HD-NNP as good agreement with DFT has been shown.

■ COMPUTATIONAL METHOD

The DFT calculations used the same computational setup that was used in an earlier AIMD study,[12] which is summarized here. A 3 × 3 Cu supercell with five layers and 13 Å vacuum distance is used, where the bottom two layers are fixed and the metal atoms in the other layers are allowed to move in order to simulate a surface temperature of 550 K. Furthermore, a plane wave cutoff of 350 eV and a 6 × 6 × 1 Γ-centered k-point grid are used. All calculations are performed with the Vienna Ab-initio Simulation Package (VASP version 5.3.5)[61−65] with the SRP32-vdW functional.[9−12,29,66−68]

DOI: 10.1021/acs.jpclett.9b00560
J. Phys. Chem. Lett. 2019, 10, 1763−1768

■ ASSOCIATED CONTENT

Supporting Information

The Supporting Information is available free of charge on the ACS Publications website at DOI: 10.1021/acs.jpclett.9b00560.

Description of the training data set and fitting error, employed symmetry functions for the HD-NNP, initial conditions of the molecular beam, elbow plots, and statistical analysis (PDF)

■ AUTHOR INFORMATION

Corresponding Authors

*E-mail: n.gerrits@lic.leidenuniv.nl.
*E-mail: g.j.kroes@chem.leidenuniv.nl.

ORCID

N. Gerrits: 0000-0001-5405-7860
Khosrow Shakouri: 0000-0002-5550-9731
Jörg Behler: 0000-0002-1220-1542
Geert-Jan Kroes: 0000-0002-4913-4689

Notes

The authors declare no competing financial interest.

■ ACKNOWLEDGMENTS

This work has been financially supported by the European Research Council through an ERC2013 advanced grant (No. 338580) and through an NWO/CW TOP Grant (No. 715.017.001). Furthermore, this work was carried out on the Dutch national e-infrastructure with the support of NWO-EW. J.B. thanks the Deutsche Forschungsgemeinschaft for a Heisenberg professorship (Be3264/11-2; Project Number 329898176).

■ REFERENCES

(1) Ertl, G. Primary Steps in Catalytic Synthesis of Ammonia. *J. Vac. Sci. Technol., A* **1983**, *1*, 1247−1253.
(2) Wei, J.; Iglesia, E. Mechanism and Site Requirements for Activation and Chemical Conversion of Methane on Supported Pt Clusters and Turnover Rate Comparisons among Noble Metals. *J. Phys. Chem. B* **2004**, *108*, 4094−4103.
(3) Kroes, G.-J. Towards Chemically Accurate Simulation of Molecule−Surface Reactions. *Phys. Chem. Chem. Phys.* **2012**, *14*, 14966−14981.
(4) Jackson, B.; Nattino, F.; Kroes, G.-J. Dissociative Chemisorption of Methane on Metal Surfaces: Tests of Dynamical Assumptions Using Quantum Models and Ab Initio Molecular Dynamics. *J. Chem. Phys.* **2014**, *141*, 054102.
(5) Wellendorff, J.; Silbaugh, T. L.; Garcia-Pintos, D.; Nørskov, J. K.; Bligaard, T.; Studt, F.; Campbell, C. T. A Benchmark Database for Adsorption Bond Energies to Transition Metal Surfaces and Comparison to Selected DFT Functionals. *Surf. Sci.* **2015**, *640*, 36−44.
(6) Gautier, S.; Steinmann, S. N.; Michel, C.; Fleurat-Lessard, P.; Sautet, P. Molecular Adsorption at Pt(111). How Accurate Are DFT Functionals? *Phys. Chem. Chem. Phys.* **2015**, *17*, 28921−28930.
(7) Kroes, G.-J. Toward a Database of Chemically Accurate Barrier Heights for Reactions of Molecules with Metal Surfaces. *J. Phys. Chem. Lett.* **2015**, *6*, 4106−4114.
(8) Füchsel, G.; Zhou, X.; Jiang, B.; Juaristi, J. I.; Alducin, M.; Guo, H.; Kroes, G.-J. Reactive and Nonreactive Scattering of HCl from Au(111): An Ab Initio Molecular Dynamics Study. *J. Phys. Chem. C* **2019**, *123*, 2287−2299.
(9) Nattino, F.; Migliorini, D.; Kroes, G.-J.; Dombrowski, E.; High, E. A.; Killelea, D. R.; Utz, A. L. Chemically Accurate Simulation of a Polyatomic Molecule-Metal Surface Reaction. *J. Phys. Chem. Lett.* **2016**, *7*, 2402−2406.
(10) Migliorini, D.; Chadwick, H.; Nattino, F.; Gutiérrez-González, A.; Dombrowski, E.; High, E. A.; Guo, H.; Utz, A. L.; Jackson, B.; Beck, R. D.; et al. Surface Reaction Barriometry: Methane Dissociation on Flat and Stepped Transition-Metal Surfaces. *J. Phys. Chem. Lett.* **2017**, *8*, 4177−4182.
(11) Chadwick, H.; Gutiérrez-González, A.; Migliorini, D.; Beck, R. D.; Kroes, G.-J. Incident Angle Dependence of CHD_3 Dissociation on the Stepped Pt(211) Surface. *J. Phys. Chem. C* **2018**, *122*, 19652−19660.
(12) Gerrits, N.; Migliorini, D.; Kroes, G.-J. Dissociation of CHD_3 on Cu(111), Cu(211), and Single Atom Alloys of Cu(111). *J. Chem. Phys.* **2018**, *149*, 224701.
(13) Behler, J.; Parrinello, M. Generalized Neural-Network Representation of High-Dimensional Potential-Energy Surfaces. *Phys. Rev. Lett.* **2007**, *98*, 146401.
(14) Behler, J. Representing Potential Energy Surfaces by High-Dimensional Neural Network Potentials. *J. Phys.: Condens. Matter* **2014**, *26*, 183001.
(15) Shakouri, K.; Behler, J.; Meyer, J.; Kroes, G.-J. Accurate Neural Network Description of Surface Phonons in Reactive Gas−Surface Dynamics: N2 + Ru(0001). *J. Phys. Chem. Lett.* **2017**, *8*, 2131−2136.
(16) Kolb, B.; Luo, X.; Zhou, X.; Jiang, B.; Guo, H. High-Dimensional Atomistic Neural Network Potentials for Molecule−Surface Interactions: HCl Scattering from Au(111). *J. Phys. Chem. Lett.* **2017**, *8*, 666−672.
(17) Shakouri, K.; Behler, J.; Meyer, J.; Kroes, G.-J. Analysis of Energy Dissipation Channels in a Benchmark System of Activated Dissociation: N2 on Ru(0001). *J. Phys. Chem. C* **2018**, *122*, 23470−23480.
(18) Hu, X.; Yang, M.; Xie, D.; Guo, H. Vibrational Enhancement in the Dynamics of Ammonia Dissociative Chemisorption on Ru(0001). *J. Chem. Phys.* **2018**, *149*, 044703.
(19) Liu, Q.; Zhou, X.; Zhou, L.; Zhang, Y.; Luo, X.; Guo, H.; Jiang, B. Constructing High-Dimensional Neural Network Potential Energy Surfaces for Gas−Surface Scattering and Reactions. *J. Phys. Chem. C* **2018**, *122*, 1761−1769.
(20) Jiang, B.; Guo, H. Dynamics of Water Dissociative Chemisorption on Ni(111): Effects of Impact Sites and Incident Angles. *Phys. Rev. Lett.* **2015**, *114*, 166101.
(21) Shen, X.; Chen, J.; Zhang, Z.; Shao, K.; Zhang, D. H. Methane Dissociation on Ni(111): A Fifteen-Dimensional Potential Energy Surface Using Neural Network Method. *J. Chem. Phys.* **2015**, *143*, 144701.
(22) Zhou, X.; Nattino, F.; Zhang, Y.; Chen, J.; Kroes, G.-J.; Guo, H.; Jiang, B. Dissociative Chemisorption of Methane on Ni(111) Using a Chemically Accurate Fifteen Dimensional Potential Energy Surface. *Phys. Chem. Chem. Phys.* **2017**, *19*, 30540−30550.
(23) Chen, J.; Zhou, X.; Zhang, Y.; Jiang, B. Vibrational Control of Selective Bond Cleavage in Dissociative Chemisorption of Methanol on Cu(111). *Nat. Commun.* **2018**, *9*, 4039.
(24) Zhang, Y.; Zhou, X.; Jiang, B. Bridging the Gap between Direct Dynamics and Globally Accurate Reactive Potential Energy Surfaces Using Neural Networks. *J. Phys. Chem. Lett.* **2019**, *10*, 1185−1191.
(25) Tiwari, A. K.; Nave, S.; Jackson, B. The Temperature Dependence of Methane Dissociation on Ni(111) and Pt(111): Mixed Quantum-Classical Studies of the Lattice Response. *J. Chem. Phys.* **2010**, *132*, 134702.
(26) Nattino, F.; Díaz, C.; Jackson, B.; Kroes, G.-J. Effect of Surface Motion on the Rotational Quadrupole Alignment Parameter of D_2 Reacting on Cu(111). *Phys. Rev. Lett.* **2012**, *108*, 236104.
(27) Mondal, A.; Wijzenbroek, M.; Bonfanti, M.; Díaz, C.; Kroes, G.-J. Thermal Lattice Expansion Effect on Reactive Scattering of H_2 from Cu(111) at T_s = 925 K. *J. Phys. Chem. A* **2013**, *117*, 8770−8781.
(28) Füchsel, G.; del Cueto, M.; Díaz, C.; Kroes, G.-J. Enigmatic HCl + Au(111) Reaction: A Puzzle for Theory and Experiment. *J. Phys. Chem. C* **2016**, *120*, 25760−25779.

DOI: 10.1021/acs.jpclett.9b00560
J. Phys. Chem. Lett. 2019, 10, 1763−1768

(29) Gerrits, N.; Kroes, G.-J. An AIMD Study of Dissociative Chemisorption of Methanol on Cu(111) with Implications for Formaldehyde Formation. *J. Chem. Phys.* **2019**, *150*, 024706.
(30) Zhou, X.; Jiang, B. A Modified Generalized Langevin Oscillator Model for Activated Gas-Surface Reactions. *J. Chem. Phys.* **2019**, *150*, 024704.
(31) Baule, B. Theoretische Behandlung Der Erscheinungen in Verdünnten Gasen. *Ann. Phys.* **1914**, *349*, 145−176.
(32) Guo, H.; Farjamnia, A.; Jackson, B. Effects of Lattice Motion on Dissociative Chemisorption: Toward a Rigorous Comparison of Theory with Molecular Beam Experiments. *J. Phys. Chem. Lett.* **2016**, *7*, 4576−4584.
(33) Frankcombe, T. J. Interpolating DFT Data for 15D Modeling of Methane Dissociation on an Fcc Metal. *Int. J. Chem. Kinet.* **2018**, *50*, 285−293.
(34) Shen, X. J.; Lozano, A.; Dong, W.; Busnengo, H. F.; Yan, X. H. Towards Bond Selective Chemistry from First Principles: Methane on Metal Surfaces. *Phys. Rev. Lett.* **2014**, *112*, 046101.
(35) Lozano, A.; Shen, X. J.; Moiraghi, R.; Dong, W.; Busnengo, H. F. Cutting a Chemical Bond with Demon's Scissors: Mode- and Bond-Selective Reactivity of Methane on Metal Surfaces. *Surf. Sci.* **2015**, *640*, 25−35.
(36) Li, X.; Cai, W.; An, J.; Kim, S.; Nah, J.; Yang, D.; Piner, R.; Velamakanni, A.; Jung, I.; Tutuc, E.; et al. Large-Area Synthesis of High-Quality and Uniform Graphene Films on Copper Foils. *Science* **2009**, *324*, 1312−1314.
(37) Losurdo, M.; Giangregorio, M. M.; Capezzuto, P.; Bruno, G. Graphene CVD Growth on Copper and Nickel: Role of Hydrogen in Kinetics and Structure. *Phys. Chem. Chem. Phys.* **2011**, *13*, 20836−20843.
(38) Zhang, W.; Wu, P.; Li, Z.; Yang, J. First-Principles Thermodynamics of Graphene Growth on Cu Surfaces. *J. Phys. Chem. C* **2011**, *115*, 17782−17787.
(39) Li, K.; He, C.; Jiao, M.; Wang, Y.; Wu, Z. A First-Principles Study on the Role of Hydrogen in Early Stage of Graphene Growth during the CH_4 Dissociation on Cu(111) and Ni(111) Surfaces. *Carbon* **2014**, *74*, 255−265.
(40) Wang, X.; Yuan, Q.; Li, J.; Ding, F. The Transition Metal Surface Dependent Methane Decomposition in Graphene Chemical Vapor Deposition Growth. *Nanoscale* **2017**, *9*, 11584−11589.
(41) Kraus, J.; Böbel, L.; Zwaschka, G.; Günther, S. Understanding the Reaction Kinetics to Optimize Graphene Growth on Cu by Chemical Vapor Deposition. *Ann. Phys.* **2017**, *529*, 1700029.
(42) Tian, B.; Liu, T.; Yang, Y.; Li, K.; Wu, Z.; Wang, Y. CH_4 Dissociation in the Early Stage of Graphene Growth on Fe−Cu(100) Surface: Theoretical Insights. *Appl. Surf. Sci.* **2018**, *427*, 953−960.
(43) Rettner, C. T.; Auerbach, D. J.; Lee, J. Dynamics of the Formation of CD_4 from the Direct Reaction of Incident D Atoms with CD_3/Cu(111). *J. Chem. Phys.* **1996**, *105*, 10115−10122.
(44) Behler, J. Atom-Centered Symmetry Functions for Constructing High-Dimensional Neural Network Potentials. *J. Chem. Phys.* **2011**, *134*, 074106.
(45) Behler, J. Constructing High-Dimensional Neural Network Potentials: A Tutorial Review. *Int. J. Quantum Chem.* **2015**, *115*, 1032−1050.
(46) Behler, J. First Principles Neural Network Potentials for Reactive Simulations of Large Molecular and Condensed Systems. *Angew. Chem., Int. Ed.* **2017**, *56*, 12828−12840.
(47) Behler, J. *RuNNer - A Neural Network Code for High-Dimensional Neural Network Potential-Energy Surfaces*. Universität Göttingen; http://www.uni-goettingen.de/de/560580.html (2018).
(48) Plimpton, S. Fast Parallel Algorithms for Short-Range Molecular Dynamics. *J. Comput. Phys.* **1995**, *117*, 1−19.
(49) Singraber, A.; Behler, J.; Dellago, C. Library-Based LAMMPS Implementation of High-Dimensional Neural Network Potentials. *J. Chem. Theory Comput.* **2019**, *15*, 1827−1840.
(50) Hundt, P. M.; Jiang, B.; van Reijzen, M. E.; Guo, H.; Beck, R. D. Vibrationally Promoted Dissociation of Water on Ni(111). *Science* **2014**, *344*, 504−507.
(51) Polanyi, J. C. Concepts in Reaction Dynamics. *Acc. Chem. Res.* **1972**, *5*, 161−168.
(52) Marcus, R. A. On the Analytical Mechanics of Chemical Reactions. Quantum Mechanics of Linear Collisions. *J. Chem. Phys.* **1966**, *45*, 4493−4499.
(53) McCullough, E. A.; Wyatt, R. E. Quantum Dynamics of the Collinear (H, H_2) Reaction. *J. Chem. Phys.* **1969**, *51*, 1253−1254.
(54) Jiang, B.; Yang, M.; Xie, D.; Guo, H. Quantum Dynamics of Polyatomic Dissociative Chemisorption on Transition Metal Surfaces: Mode Specificity and Bond Selectivity. *Chem. Soc. Rev.* **2016**, *45*, 3621−3640.
(55) Juurlink, L. B. F.; Killelea, D. R.; Utz, A. L. State-Resolved Probes of Methane Dissociation Dynamics. *Prog. Surf. Sci.* **2009**, *84*, 69−134.
(56) Schmid, M. P.; Maroni, P.; Beck, R. D.; Rizzo, T. R. Surface Reactivity of Highly Vibrationally Excited Molecules Prepared by Pulsed Laser Excitation: CH_4 ($2\nu_3$) on Ni(100). *J. Chem. Phys.* **2002**, *117*, 8603−8606.
(57) Guo, H.; Jackson, B. Mode-Selective Chemistry on Metal Surfaces: The Dissociative Chemisorption of CH_4 on Pt(111). *J. Chem. Phys.* **2016**, *144*, 184709.
(58) Farjamnia, A.; Jackson, B. The Dissociative Chemisorption of Water on Ni(111): Mode- and Bond-Selective Chemistry on Metal Surfaces. *J. Chem. Phys.* **2015**, *142*, 234705.
(59) Campbell, V. L.; Chen, N.; Guo, H.; Jackson, B.; Utz, A. L. Substrate Vibrations as Promoters of Chemical Reactivity on Metal Surfaces. *J. Phys. Chem. A* **2015**, *119*, 12434−12441.
(60) Spiering, P.; Wijzenbroek, M.; Somers, M. F. An Improved Static Corrugation Model. *J. Chem. Phys.* **2018**, *149*, 234702.
(61) Kresse, G.; Hafner, J. Ab Initio Molecular-Dynamics Simulation of the Liquid-Metal−Amorphous-Semiconductor Transition in Germanium. *Phys. Rev. B: Condens. Matter Mater. Phys.* **1994**, *49*, 14251−14269.
(62) Kresse, G.; Hafner, J. Ab Initio Molecular Dynamics for Liquid Metals. *Phys. Rev. B: Condens. Matter Mater. Phys.* **1993**, *47*, 558−561.
(63) Kresse, G.; Furthmüller, J. Efficient Iterative Schemes for Ab Initio Total-Energy Calculations Using a Plane-Wave Basis Set. *Phys. Rev. B: Condens. Matter Mater. Phys.* **1996**, *54*, 11169−11186.
(64) Kresse, G.; Furthmüller, J. Efficiency of Ab-Initio Total Energy Calculations for Metals and Semiconductors Using a Plane-Wave Basis Set. *Comput. Mater. Sci.* **1996**, *6*, 15−50.
(65) Kresse, G.; Joubert, D. From Ultrasoft Pseudopotentials to the Projector Augmented-Wave Method. *Phys. Rev. B: Condens. Matter Mater. Phys.* **1999**, *59*, 1758−1775.
(66) Migliorini, D.; Chadwick, H.; Kroes, G.-J. Methane on a Stepped Surface: Dynamical Insights on the Dissociation of CHD_3 on Pt(111) and Pt(211). *J. Chem. Phys.* **2018**, *149*, 094701.
(67) Chadwick, H.; Migliorini, D.; Kroes, G. J. CHD_3 Dissociation on Pt(111): A Comparison of the Reaction Dynamics Based on the PBE Functional and on a Specific Reaction Parameter Functional. *J. Chem. Phys.* **2018**, *149*, 044701.
(68) Migliorini, D.; Nattino, F.; Tiwari, A. K.; Kroes, G.-J. HOD on Ni(111): Ab Initio Molecular Dynamics Prediction of Molecular Beam Experiments. *J. Chem. Phys.* **2018**, *149*, 244706.

DOI: 10.1021/acs.jpclett.9b00560
J. Phys. Chem. Lett. 2019, 10, 1763−1768